Cytokine 114 (2019) 106–114

Contents lists available at ScienceDirect

Cytokine

journal homepage: www.elsevier.com/locate/cytokine

Molecular characterization of the 2′,5′-oligoadenylate synthetase family in the Chinese tree shrew (*Tupaia belangeri chinensis*)

Yu-Lin Yao[a,b], Dandan Yu[a,c], Ling Xu[a,c], Yu Fan[a,c], Yong Wu[a,b], Tianle Gu[a,b], Jiaqi Chen[d], Long-Bao Lv[d], Yong-Gang Yao[a,b,c,d,*]

[a] Key Laboratory of Animal Models and Human Disease Mechanisms of Chinese Academy of Sciences & Yunnan Province, Kunming Institute of Zoology, Kunming, Yunnan 650223, China
[b] Kunming College of Life Science, University of Chinese Academy of Sciences, Kunming, Yunnan 650223, China
[c] Center for Excellence in Animal Evolution and Genetics, Chinese Academy of Sciences, Kunming 650223, China
[d] Kunming Primate Research Center of the Chinese Academy of Sciences, Kunming Institute of Zoology, Chinese Academy of Sciences, Kunming 650223, China

ARTICLE INFO

Keywords:
OAS
Chinese tree shrew
Virus infection
RNase L
Innate immunity

ABSTRACT

Virus infection induces type I interferons (IFNs) that in turn exert their pleiotropic effects through inducing a large number of interferon-stimulated genes (ISGs). The IFN-induced 2′,5′-oligoadenylate synthetases (OASs) have been identified as a member of the ISGs family characterized by the ability to synthesize 2′,5′-oligoadenylate (2-5A), which can induce the degradation of viral RNA by activating RNase L within the infected cells to block viral replications. In this study, we characterized the *OASs* of the Chinese tree shrew (*Tupaia belangeri chinensis*), a small mammal genetically close to primates and has the potential as animal model for viral infections. We identified 4 putative tree shrew *OASs* (*tOASs*, including *tOAS1*, *tOAS2*, *tOASL1*, and *tOASL2*) and characterized their roles in antiviral responses. Tree shrew lost *tOAS3* that was presented in human and mouse. Phylogenetic analyses based on the protein sequences showed a close relationship of tOASs with those of mammals. Constitutive mRNA expression of *tOASs* was found in seven tissues (heart, liver, spleen, lung, kidney, small intestine and brain). Moreover, *tOASs* were significantly up-regulated upon various virus infections. Overexpression of *tOASs* significantly inhibited DNA virus and RNA virus replications in tree shrew primary renal cells. tOAS1 and tOAS2, but not tOASL1 and tOASL2, exerted their anti-HSV activity in an RNase L-dependent pathway. Collectively, our results revealed the evolutionary conservation of *tOASs* in tree shrew and might offer helpful information for creating viral infection models using the Chinese tree shrew.

1. Introduction

The Chinese tree shrew (*Tupaia belangeri chinensis*) belongs to the order Scandentia and emerges as a viable alternative animal model for biomedical research due to its unique characteristics, such as small adult body size, high brain-to-body mass ratio, short reproductive cycle and life span, low cost of maintenance, and most importantly, a closer affinity to primates [1–6]. This animal is widely distributed in Southeast Asia and Southwest China [1,7]. Tree shrew has susceptibility to a wide variety of human pathogens, such as hepatitis B virus [8–10], hepatitis C virus [11], herpes simplex virus [12,13], Coxsackie virus [14], influenza virus [15] and bacteria [16,17]. It was also used for creating animal models for breast cancer [18], basal cell carcinoma [19], non-alcoholic fatty liver disease [20], and Alzheimer's disease [21], to name a few. With the successful creation of transgenic tree shrew [22], we would expect a boost of researches using this animal in biomedical research [5].

Since the determination of genome of the Chinese tree shrew [2], we found that the innate immune system, which acts as the first line of defense against invading pathogens [23,24], harbored several unique features in the Chinese tree shrew [2,25,26]. Normally, the antiviral innate immune responses are triggered by the detection of microbial pathogens through a set of pattern-recognition receptors (PRRs) in the host [24], and toll-like receptors, retinoic acid-inducible gene-I-like receptors, nucleotide-binding oligomerization domain-like receptors and cytoplasmic DNA sensors serve as PRRs to recognize various viral structural components [27]. After detection of invading viruses, the host cells activate a series of signaling events to induce IFNs, which

* Corresponding author at: Key Laboratory of Animal Models and Human Disease Mechanisms of Chinese Academy of Sciences & Yunnan Province, Kunming Institute of Zoology, Kunming, Yunnan 650223, China.
E-mail address: yaoyg@mail.kiz.ac.cn (Y.-G. Yao).

https://doi.org/10.1016/j.cyto.2018.11.009
Received 8 September 2018; Received in revised form 9 November 2018; Accepted 10 November 2018
Available online 20 November 2018

initiate a signaling cascade to regulate numerous antiviral genes to help the host cells against the invading viruses [23,24,28]. The Chinese tree shrew contains no retinoic acid-inducible gene-I (RIG-I) and this leads to a functional replacement with melanoma differentiation factor 5 (MDA5) to sense the invading pathogens [25]. Moreover, TLR10 becomes a pseudogene in this animal [26]. Whether there are any specialties for the interferon-stimulated genes (ISGs) in the Chinese tree shrew to cope with the evolutionary changes in the retinoic acid inducible gene I (RIG-I)-like receptor (RLR) and Toll-like receptor (TLR) pathways remain to be determined.

The 2′,5′- oligoadenylate synthetases, a family of ISGs, are induced by type I and type II IFNs. Human has 4 functional OAS family members (hOAS1, hOAS2, hOAS3, and hOASL that was termed as hOAS-like) [29], whereas mouse has 5 functional OASs (mOas1, mOas2, mOas3, mOasl1 and mOalsl2) [30]. As cellular PRRs, OAS proteins are activated by viral double-stranded RNA (dsRNA) [31]. Once stimulated by viral dsRNA, active OASs use ATP to synthesize 2′-5′ oligoadenylates (2-5A) [30,32,33]. The 2-5As activate RNaseL by inducing its dimerization and then induce the degradation of viral and cellular RNAs, including rRNA and mRNA, subsequently to a drop in global protein synthesis, thus resulting in the inhibition of viral replications [33–36]. OAS family proteins belong to an ancient nucleotidyltransferase (NTase) superfamily [33]. Previous studies have shown that NTase domain and OAS domain are obviously related to the OAS enzyme activity [37,38]. The NTase domains contain two OAS-specific motifs: P-loop and D-box motifs, which are involved in ATP binding and Mg^{2+}, respectively [37,39,40]. Mutational studies have demonstrated that the Gly-Ser pattern (GS) in the P-loop motif and Asp pattern (D-D) in the D-box motif are important for the OAS enzyme activity [37,39]. A tripeptide motif (CFK) within the OAS domains has been reported to mediate the oligomerization of 2-5A, but may not be essential for the OAS enzyme activity [41]. Among them, OAS1-OAS3 possess the ability to synthesize 2-5A and exert the antiviral activity via the canonical RNase L dependent pathway, while hOASL and mOasl1 lack the ability to synthesize 2-5A [38,42]. hOASL promotes host antiviral activity by enhancing RIG-I activation [43], but mOasl1 specifically binds to IRF7 5′UTR and inhibits the translation of *IRF7* mRNA, thus negatively regulating the antiviral innate immunity [44]. The OAS/RNase L system, an IFN-induced antiviral innate immune pathway, plays a critical role in blocking viral infections [31], and has attracted accumulating attention on therapeutic strategies for constraining pathogenic viruses [45]. A better understanding of the OAS family, as a typical case for understanding the role of ISGs in the Chinese tree shrew, may offer new insights into the development of animal model for virus infections.

In this study, we obtained the full-length cDNA of the OAS family genes of the Chinese tree shrew and detected their expression pattern in different tissues and primary renal cells in response to viral challenges. We further tested whether tOAS family proteins exerted their antiviral activity in an RNaseL dependent pathway. Our results demonstrated that tOAS family genes were highly conserved in evolution and had antiviral activity to a variety of viruses.

2. Materials and methods

2.1. Experimental animals, tissues and cells

The healthy adult Chinese tree shrews (n = 5) were introduced from the experimental animal core facility of the Kunming Primate Research Center, Kunming Institute of Zoology (KIZ), Chinese Academy of Sciences (CAS). We collected seven different tissues, including heart, liver, spleen, lung, kidney, small intestine and brain from each animal after euthanasia. Tissues were immediately frozen in liquid nitrogen for storage. Tree shrew primary renal cells (TSPRCs) were prepared according to the procedure described in our previous studies [26,46,47]. Cells were cultured at 37 °C in 5% CO_2 with Dulbecco's modified Eagle medium (DMEM) supplemented with 10% fetal bovine serum (FBS) and 1 × penicillin/streptomycin (Invitrogen, USA). All experimental procedures were performed with the approval of the Institutional Animal Care and Use Committee of the KIZ.

2.2. RNA extraction and expression quantification

Total RNA from seven tissues and TSPRCs were extracted using the RNAsimple Total RNA Kit (TIANGEN, Beijing) according to the manufacturer's instruction. The quality of total RNA was measured on a biophotometer (Eppendorf). About 2 μg total RNA (with an A260/A280 ratio of 1.8–2.0) was used to synthesize cDNA by using oligo-dT_{18} primer and M-MLV reverse transcriptase (Promega, USA). Reverse transcription quantitative real-time PCR (RT-qPCR) was conducted using iTaq Universal SYBR Green Supermix (BioRad, USA) with gene specific primer pairs (Table S1) on a MyIQ2 Two-Color Real-Time PCR Detection system (Bio-Rad, USA). The thermal cycling protocol was 1 cycle at 95 °C for 1 min, 40 cycles of 95 °C for 15 s and 55 °C for 15 s. The tree shrew *β-actin* transcript was amplified by gene specific primer pair [47] for the normalization of the target gene.

2.3. Cloning of the full-length tOASs

Four *tOASs* could be predicted according to the genome sequence of the Chinese tree shrew described in our previous study [2] and were retrieved from the tree shrew database (http://www.treeshrewdb.org) [48]. To get the relatively intact mRNA sequences of the tOASs, the 5′ UTR and 3′ UTR were obtained by rapid amplification of cDNA ends (RACE) using the SMARTer RACE cDNA Amplification Kit (Clontech, USA) and 3′ Full RACE Core Set Ver.2.0 (TaKaRa, Japan), respectively, and the coding region was amplified by using specific primer pairs (Table S1). Purified PCR and RACE products were cloned into the PMD 19-T simple vector (TaKaRa, Dalian, China). Five positive clones of each insert were sequenced to get a consensus sequence.

2.4. Virus infections

Herpes simplex virus-1 (HSV-1), Sendai virus (SeV), Newcastle disease virus (NDV), vesicular stomatitis virus (tagged by GFP; VSV-GFP), and avian influenza virus (AIV) were taken from our previous studies [25,46,47]. For virus infection, TSPRCs were washed three times in phosphate-buffered saline (PBS) and were incubated with the indicated virus for 1 h in DMEM without FBS. Cells were rinsed with PBS and cultured with fresh DMEM containing 1% FBS as described in our recent studies [25,47].

2.5. Plasmid construction, transfection, and western blotting analysis

The open reading frame (ORF) of each *tOAS* was subcloned into FLAG-tagged pCMV-3Tag-8 with *Not* I and *Eco*R V to generate overexpression vector. All constructs were confirmed by sequencing. TSPRCs were transfected with the indicated expression vectors or siRNAs targeting *tRNase L* mRNA (RiboBio, Guangzhou, China) for 48 h using the X-treme GENE HP DNA Transfection Reagent (Roche; 06366546001). Cells were then harvested and lysed on ice in RIPA lysis buffer (Beyotime Institute of Biotechnology; P0013).

A total of 20 μg cellular proteins were used for Western blotting. Briefly, each protein sample was subjected to 12% SDS-PAGE, then transferred onto polyvinylidene fluoride (PVDF) membranes (Roche) using the standard procedure. The PVDF membranes were blocked in 5% nonfat dry milk dissolved in Tris-buffered saline (TBS) containing 0.1% Tween 20 (TBST) at room temperature for 2 h. The membranes were incubated with respective antibody (mouse anti-FLAG (1:5000, EnoGene) or mouse anti GAPDH (1:10000, EnoGene)) overnight at 4 °C. The membranes were washed three times (5 min each time) with TBST and were incubated with anti-mouse secondary antibody (1:10000, KPL, USA) for 1 h at room temperature. After washing, protein bands on

the membrane were visualized using the enhanced chemiluminescence (ECL) reagents (Millipore).

2.6. Immunofluorescence staining

TSPRCs were seeded on glass coverslips and transfected with the indicated vectors for 36 h, then cells were left uninfected or infected with HSV-1 (multiplicity of infection (MOI) = 1) and NDV (MOI = 1) for 12 h. After a brief wash with PBS, cells were fixed with 300 μL 4% paraformaldehyde (PFA) for 15 min at 37 °C, then were washed three times (5 min each time) with PBS and permeabilized with 0.1% Triton X-100 (Sigma-Aldrich) for 15 min at room temperature. After another round of three washes (5 min each time) with PBS, the slides were blocked with 5% bovine serum albumin for 30 min at room temperature. The fixed cells were incubated with mouse anti-FLAG (1:500, EnoGene) overnight at 4 °C. After washing with PBS three times, cells were incubated with the FITC-conjugated secondary antibody (1:500, Life Technologies) at room temperature for 2 h. The nuclei were stained with 1 μg/mL DAPI (Roche) for 15 min at room temperature. The slides were visualized using an Olympus FluoView™ 1000 confocal microscope (Olympus, Germany).

2.7. Phylogenetic analysis and positive selection

We inferred the phylogenetic position of the Chinese tree shrew based on the *OAS* family genes from 10 vertebrate species (Table S2): *Homo sapiens* (human), *Pan troglodytes* (chimpanzee), *Macaca mulatta* (rhesus monkey), *Sus scrofa* (pig), *Ovis aries* (sheep), *Bos taurus* (cattle), *Canis lupus familiaris* (dog), *Myotis lucifugus* (bat), *Mus musculus* (mouse), *Rattus norvegicus* (rat). The protein sequences were aligned by the ClustalW method using Muscle 3.8 software [49], with the guidance of aligned sequences. Phylogenetic trees for each gene and genes of the entire *OAS* family were constructed using the neighbor-joining (NJ) method and the maximum likelihood (ML) by MEGA6.0 [50], respectively. *Myotis lucifugus* was used as the outgroup to root single gene trees. Each tree was supported by 1000 bootstrap replications to determine the confidence of tree branch positions.

To detect potential positive selection on the *OAS* family genes in the tree shrew lineage, we used single copy orthologous genes of *OASs* (including *OAS2* and *OASL1*) in six mammals (human, rhesus monkey, Chinese tree shrew, rat, mouse, and dog), as described in our previous studies [21,25,26,51]. Briefly, the aligned coding regions (CDS) of *OAS2* and *OASL1* were used to calculate the non-synonymous substitution/synonymous substitution rate (dN/dS, also referred to as ω) using CODEML program implemented in the PAML package [52]. The branch-site model with likelihood ratio test (LRT) [53] was performed to test whether a proportion of sites in the sequence had a statistically significant support for $\omega > 1$ in the Chinese tree shrew lineage.

2.8. Statistical analysis

All mRNA expression data were analyzed using the GraphPad software (GraphPad Software, Inc., CA, USA) with unpaired Student's *t* test to determine the statistical significance of differences. Data were presented as mean ± SEM. A P value of < 0.05 was considered to be statistically significant.

3. Results

3.1. Cloning and evolutionary analysis of the tOASs

Human OAS family contains 4 genes (*hOAS1*, *hOAS2*, *hOAS3* and *hOASL*) and a pseudogene *hOASL2* [38]. Mouse OAS family has 5 members including *mOas1*, *mOas2*, *mOas3*, *mOasl1* and *mOasl2*. Furthermore, *mOas1* has 8 copies and their antiviral roles have been broadly recognized [33,54,55]. Based on the genome sequence of the Chinese tree shrew [2], we successfully cloned 4 *OAS* family genes (*tOAS1*, *tOAS2*, *tOASL1* and *tOASL2*) in this animal (Table 1). The Chinese tree shrew *OAS* family genes had a considerably high sequence identity with those of *hOAS* family genes. The tOAS1, tOAS2 and tOASL1 proteins shared 71.3%, 67.2%, and 75.4% residue identity to those of human orthologs, respectively (Tables S3–S5). Multiple sequence alignments and prediction for domains using the SMART program [56] showed that there were conserved motifs and domains in the sequence of tOASs, including the P-loop motifs, D-box motifs, CFK motif, NTase domains, OAS domains and ubiquitin-like domains (UBL). tOAS1 and tOAS2 contained an NTase domain but had one and two OAS units, respectively. Different from tOAS1 and tOAS2, tOASL1 and tOASL2 had two tandem UBL domains in the C-terminus (Fig. S1). Furthermore, the NTase active-site residues (GS) in the P-loop and D-box (D-D) motifs were also conserved in tOASs proteins (Fig. 1). Although we designed 6 different primer pairs (Table S1), which could form 12 combinations of primer pairs, to amplify *OAS3* based on the conserved regions between human and mouse using cDNA from TSPRCs, we obtained no amplification of *tOAS3* (Fig. S2), which suggested that Chinese the tree shrew lacks this gene. Further check with the Chinese tree shrew genome sequence that was generated using the third-generation sequencing technologies confirmed the absence of this gene in this animal (authors' unpublished data).

Table 1
Information of the full-length *OASs* in the Chinese tree shrew.

Gene	Full length, bp	5′-UTR, bp	CDS, bp (peptide, aa)	3′-UTR, bp	GenBank accession number
tOAS1	1494	60	1095 (364)	339	MH512001
tOAS2	2418	72	2082 (693)	264	MH512002
tOASL1	2176	25	1545 (514)	606	MH512003
tOASL2	2107	195	1521 (506)	391	MH512004

To gain an insight into the evolutionary relationship of the Chinese tree shrew with other mammals, phylogenetic tree using the ML method was constructed based on the OAS protein sequences. Five OAS clades were recognized in the tree (Fig. 2), which reinforced the notion that tOASs are true orthologs. Similar clustering pattern was observed in the NJ tree (Fig. S3). Interestingly, *tOAS1* and *tOAS2* were first clustered with the corresponding orthologs of primates relative to rodents, whereas *tOASL1* showed a different clustering pattern (Figs. 2 and S4).

We evaluated the evolutionary selective pressure on single copy orthologous genes of *OASs* (including *OAS2* and *OASL1*) in six mammals (human, rhesus monkey, Chinese tree shrew, rat, mouse, and dog). We found that *tOAS2* and *tOASL1* had undergone no positive selection in the Chinese tree shrew lineage (*tOAS2*, $P = 0.189$; *tOASL1*, $P = 1.000$; Table S6). Taken together, these results indicated that the *OAS* family genes are highly conserved in the Chinese tree shrew.

3.2. Tissue-specific expression of the tOAS family genes

We measured the mRNA levels of *tOASs* in seven tissues from healthy adult tree shrews. The *tOAS* mRNAs were ubiquitously detected in all tissues, with a tissue-specific pattern (Fig. 3). In particular, *tOAS1* had a relatively high mRNA level in liver, spleen, lung, and small intestine, whereas brain, kidney and heart tissues had a lower level of *tOAS1* mRNA. The mRNA levels of *tOASL1* were generally at a lower level in nearly all tissues, but liver and small intestine tissues had a relatively high level of *tOASL1* mRNA expression. The *tOASL2* mRNA was expressed at a low level in all tissues. When the mRNA expression levels of all *tOASs* were compared together, *tOAS1* and *tOAS2* had a relatively higher basal expression level than *tOASL1* and *tOASL2* in nearly all tissues (Fig. 3). The tissue-specific expression pattern of *tOASs* would suggest their different roles in the immune system.

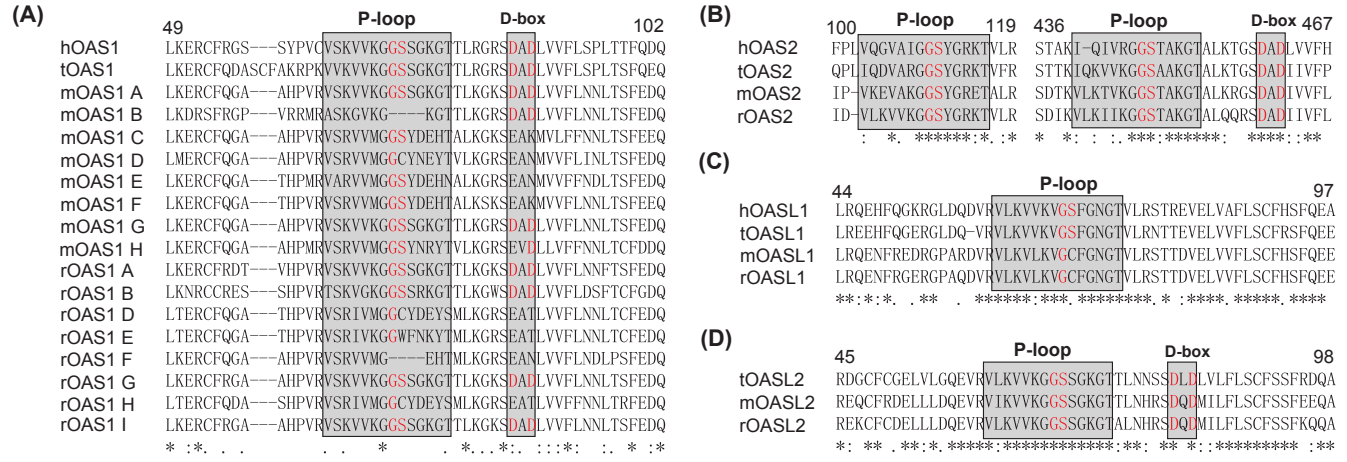

Fig. 1. Multiple sequence alignment of the P-loop and D-box motifs of the OAS family proteins. (A) Alignment of the P-loop and D-box amino acids of the OAS1 from human (hOAS1), tree shrew (tOAS1), mouse (mOAS1) and rat (rOAS1). Different copies of *OAS1* in rat (copies A, B, D–I) and mouse (copies A–H) were designated by adding suffixes of capitalized characters. (B–D) Alignment of the P-loop and D-box amino acids of the OAS2 (B), OASL1 (C) and OASL2 (D) from human, tree shrew, mouse and rat. GenBank accession numbers of the respective sequences were listed in Table S2. The identical residues among all aligned sequences were indicated as '*' and similar amino acids were indicated as ':'. The grey boxes indicated the conserved P-loop and D-box motifs. The critical residues in the motifs were highlighted by red.

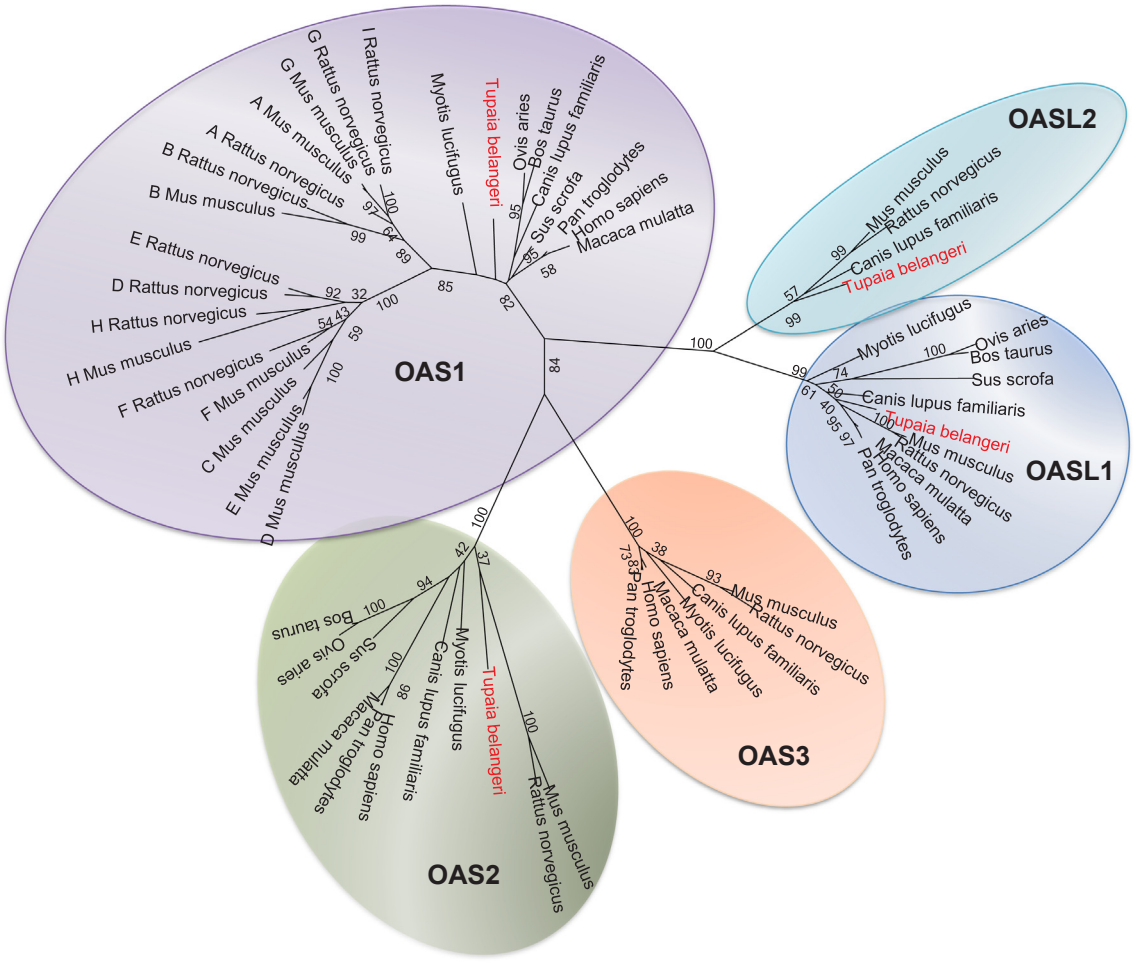

Fig. 2. Phylogenetic tree of the *OAS* family genes based on the predicted proteins of 11 mammalian species. Phylogenetic tree was reconstructed according to the Maximum likelihood (ML) method, with 1000 bootstrap replications. The bootstrap values larger than 30% are indicated on the branches. The GenBank accession numbers for the *OAS* family genes in *Homo sapiens* (human), *Pan troglodytes* (chimpanzee), *Macaca mulatta* (rhesus monkey), *Sus scrofa* (pig), *Ovis aries* (sheep), *Bos taurus* (cattle), *Canis lupus familiaris* (dog), *Myotis lucifugus* (bat), *Mus musculus* (mouse), *Rattus norvegicus* (rat), and *Tupaia belangeri chinesis* (Chinese tree shrew) were listed in Table S2. Different copies of *OAS1* in rat (copies A, B, D–I) and mouse (copies A–H) were designated by adding prefixes of capitalized characters.

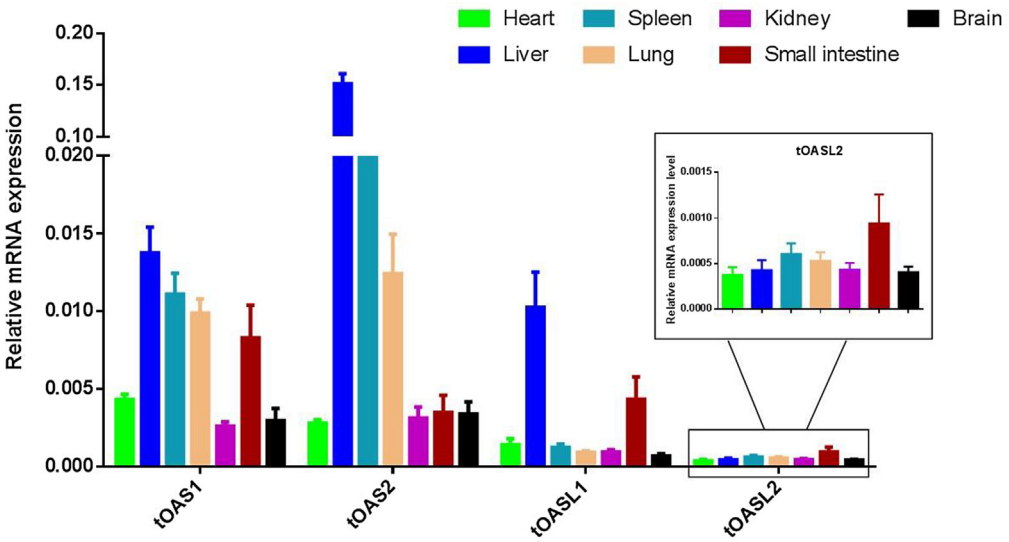

Fig. 3. mRNA expression pattern of *tOASs* in different tissues of the Chinese tree shrews. The *tOASs* mRNA expression were measured by RT-qPCR with gene-specific primers (Table S1) in seven tissues of the Chinese tree shrews (n = 5). The *β-actin* gene was used for normalization.

3.3. tOASs were upregulated by virus infections

The OASs are IFN-induced antiviral enzymes that can inhibit virus replication through the RNase L–dependent or independent pathway [31,43]. We examined the alterations of *tOAS* mRNA levels in response to different viral infections in TSPRCs. Consistent with late induction of *tIFNB1* mRNA expression that was caused by the absence of RIG-I as described in our previous study [25], we also observed a late upregulation of *tOAS* mRNA expression in TSPRCs with HSV-1 infection (Fig. 4A). The mRNA levels of all 4 *tOASs* were significantly increased in cells with infection of DNA virus (HSV-1) or RNA virus (SeV, NDV, VSV and AIV) for 12 h compared with non-infected cells (Fig. 4). Upon same RNA virus infection, the induced mRNA levels of *tOAS1* and *tOAS2* were much higher than those of *tOASL1* and *tOASL2* (Fig. 4B). These observations suggested that tOAS1 and tOAS2 might be more actively involved in antiviral immune responses than tOASL1 and tOASL2.

Subcellular localization of activated OAS protein within the cells plays active roles in antiviral responses [57]. We further determined subcellular localization of overexpressed tOASs in TSPRCs with and without virus infections. Cells without transfection were used as a negative control (Fig. S5). We found that the tOASs were diffusedly distributed in the cytoplasm. Infection of HSV-1 or NDV did not affect subcellular localization of tOASs (Fig. 5). Previous study showed that

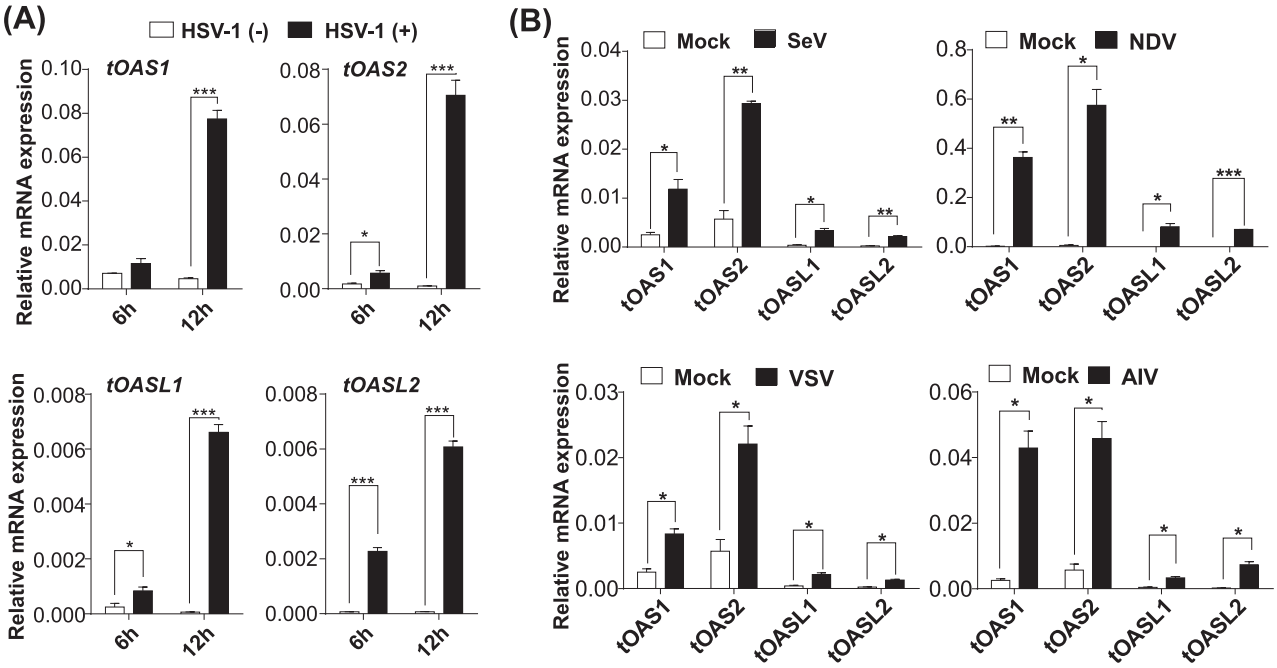

Fig. 4. mRNA expression levels of *tOASs* in the Chinese tree shrew primary renal cells (TSPRCs) in response to virus infection. (A) Upregulation of *tOAS* mRNA levels in TSPRCs upon HSV-1 infection. Cells (1×10^5/well) were grown in 24-well plate and infected with HSV-1 (MOI = 10) for 6 h and 12 h before the harvest. (B) Upregulation of mRNA levels of *tOASs* in TSPRCs with and without infection of RNA virus. Cells were infected with the indicated RNA viruses (SeV, 20 HAU/mL; NDV, MOI = 10; VSV, MOI = 0.01; AIV, MOI = 10) for 12 h. The mRNA levels of *tOAS1*, *tOAS2*, *tOASL1*, and *tOASL2* were measured by using RT-qPCR. Results were normalized to the *β-actin* gene. The data were representative of three independent experiments. Values were presented as mean ± SEM. * $P < 0.05$, ** $P < 0.01$, *** $P < 0.001$, two-tailed unpaired Student's *t*-test.

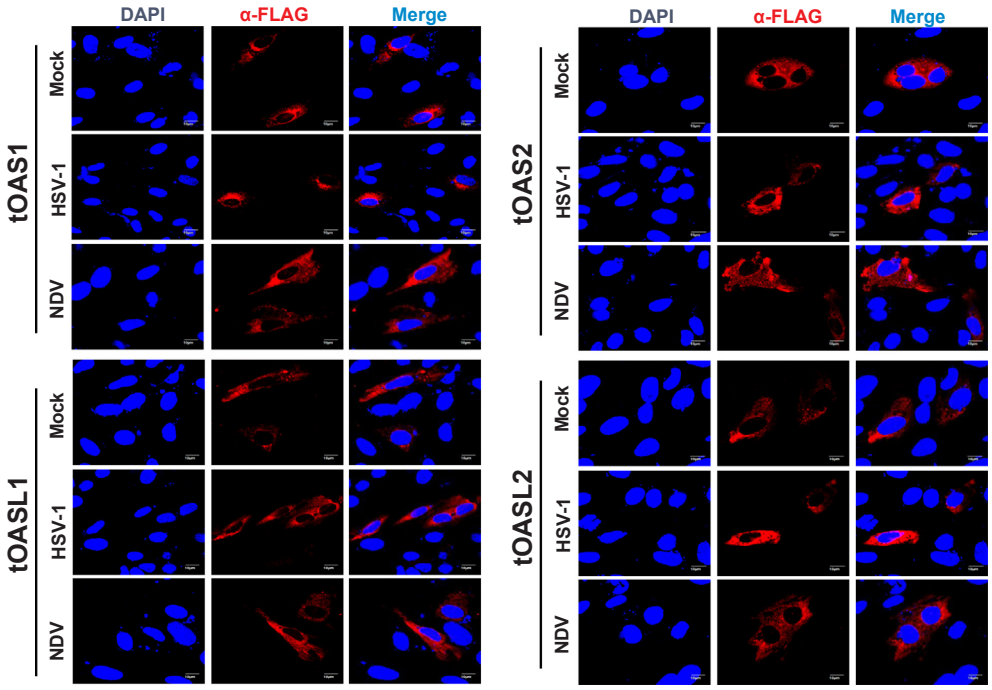

Fig. 5. Subcellular localization of overexpressed tOASs in tree shrew primary renal cells. Cells were transiently transfected with the indicated expression vector (tOAS1-FLAG, tOAS2-FLAG, tOASL1-FLAG, and tOASL2-FLAG) for 36 h, then were infected with or without HSV-1 (MOI = 1) and NDV (MOI = 1) for 12 h. Cells were stained with anti-FLAG. Nuclei were stained with blue staining (DAPI). The scale is 10 μm. Similar results were obtained from three independent experiments.

human OAS proteins were mainly distributed in the cytoplasm with dengue virus infection, but hOAS2 would have perinuclear localization after dengue virus infection [58].

3.4. tOASs played an antiviral role during virus infection

To examine the effect of the tOASs on virus replication, we overexpressed tOASs in TSPRCs and investigated their functions in suppressing viral replication. All 4 tOASs could be successfully overexpressed in TSPRCs, albeit at different levels of amount (Fig. 6A). Note that there were two bands in the Western blot for overexpression of tOAS2, and the corrected size of this protein should be 79 kDa (Fig. 6A).

Overexpression of the tOASs could significantly decrease the HSV-1 copy in TSPRCs relative to cells transfected with empty vector (Fig. 6B). Similarly, ectopic expression of tOAS1 and tOAS2 in TSPRCs significantly inhibited the replication of VSV-GFP, whereas overexpression of tOASL1 and tOASL2 had no such a significant inhibition effect (Fig. 6C). Collectively, all 4 tOASs played a critical antiviral role in HSV-1 infection, but tOAS1 and tOAS2 had a better inhibition effect than those of tOASL1 and tOASL2 for counteracting RNA virus.

3.5. The anti-HSV-1 activity of tOASL1 and tOASL2 was independent of the RNase L

OASs are able to synthesize 2-5A and regulate the early phase of viral infection by degrading viral RNA through the classical OAS/RNase L pathway, resulting in the inhibition of virus replications [33,59]. Human OASL has no enzyme activity to synthesize 2-5A, but exerts its antiviral activity via enhancing the RIG-I activity [43]. To investigate whether the antiviral effect of tOASs was dependent or independent on the RNase L, we knocked down the *tRNase L* mRNA expression in TSPRCs using three siRNAs targeting this gene (Fig. 7A). Among the three siRNA, sitRNase L-3 had the highest efficiency for reducing the endogenous *tRNase L* mRNA in TSPRCs. This siRNA was then used for

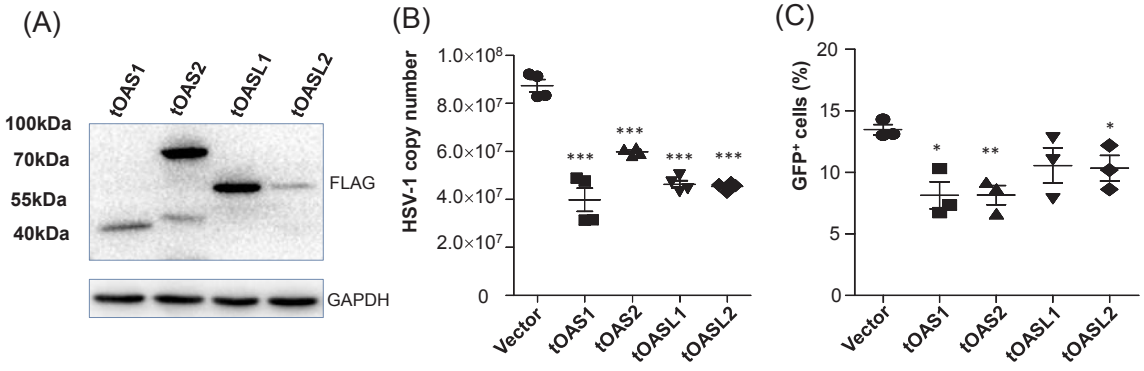

Fig. 6. Antiviral effect of tOASs in response to HSV-1 and VSV infections in the Chinese tree shrew primary renal cells. (A) Successful overexpression of tOASs in TSPRCs transfected with the indicated expression vectors for 48 h. (B) Overexpression of tOASs inhibited HSV-1 replication. Cells (1×10^5/well) were transfected with the indicated expression vector (tOAS1-FLAG, tOAS2-FLAG, tOASL1-FLAG, tOASL2-FLAG; each 1 μg) or empty vector (1 μg) for 24 h, followed by infection with HSV-1 (MOI = 10) for 1 h. Cells were washed with DMEM for 3 times and switched to culture medium for growth for 23 h. Then, the culture medium was collected to quantify the HSV-1 DNA copies by using RT-qPCR. (C) Effects of tOASs overexpression on VSV replication. Cells were transfected using the same procedure as (B) for 12 h, followed by infection with VSV-GFP (MOI = 0.01) for 12 h. Percentage of VSV-GFP positive cells was quantified using flow cytometry. Difference of inhibition effect between cells overexpressing tOAS and cells transfected with empty vector (Vector) was evaluated by using unpaired Student's *t* test. * $P < 0.05$, ** $P < 0.01$, *** $P < 0.001$. Bars represent mean ± SEM. Shown data are representative of three independent experiments with similar result.

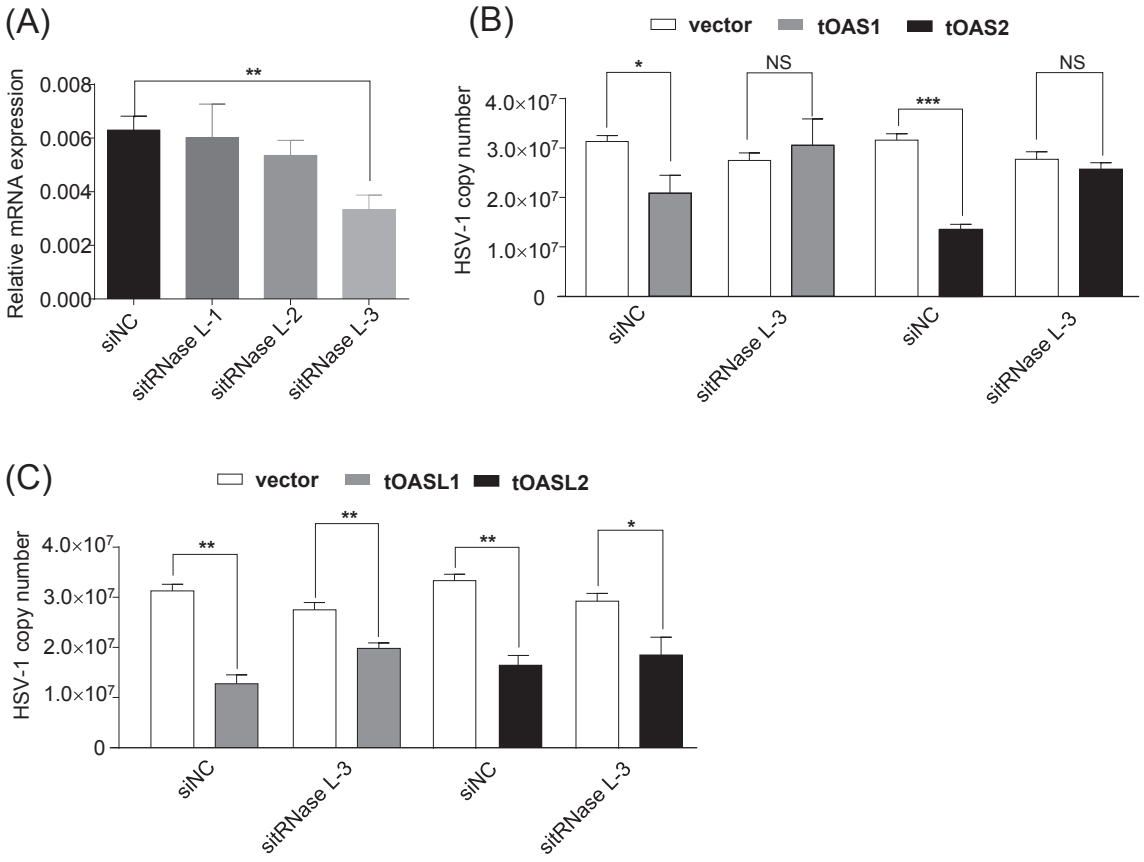

Fig. 7. Knockdown of the tRNase L affected antiviral activities of tOAS1 and tOAS2, but not tOASL1 and tOASL2, in the Chinese tree shrew primary renal cells upon HSV-1 infection. (A) Knockdown efficiency of siRNA for the tRNase L in TSPRCs. Cells (1×10^5/well) were transfected with siRNA negative control (siNC) or siRNA targeting *tRNase L* (sitRNase L-1, sitRNase L-2 and sitRNase L-3; 50 nM each) for 36 h before harvest for quantification of the *tRNase L* mRNA level. The knockdown efficiency of endogenous *tRNase L* mRNA levels was analyzed by using qRT-PCR, with normalization to the *β-actin*. Knockdown of tRNase L abolished the suppression effect on HSV-1 replication in TSPRCs overexpressing tOAS1 and tOAS2 (B), but not tOASL1 and tOASL2 (C). Cells (1×10^5/well) were co-transfected with the indicated expression vector (empty vector, tOAS1-FLAG, tOAS2-FLAG, tOASL1-FLAG and tOASL2-FLAG; each 1 μg) and siRNA (siNC and sitRNase L-3, each 50 nM) for 24 h, followed by infection with or without HSV-1 (MOI = 1) for 24 h before the harvest. NS, non-significant, * $P < 0.05$, ** $P < 0.01$, *** $P < 0.001$, Student's *t* test. Bars represent mean ± SEM. All experiments were repeated three times with similar results.

the subsequent assays. TSPRCs were transfected with sitRNase L or siNC (siRNA negative control), followed by infection with HSV-1. Knockdown of *tRNase L* dramatically reduced the anti-HSV-1 activity of tOAS1 and tOAS2 (Fig. 7B), but did not affect the anti-viral effect of tOASL1 and tOASL2 (Fig. 7C). Consistent with previous studies [33,43], our results indicated that the anti-HSV-1 activities of tOAS1 and tOAS2 are dependent on the canonical RNase L pathway, whereas those of tOASL1 and tOASL2 are independent on the RNase L pathway.

4. Discussion

Virus infection in mammals often triggers the IFN-mediated transcription of a variety of ISGs to confer antiviral activity [60]. The OASs are such kinds of IFN-inducible ISGs and are the first proteins to be identified as being involved in cellular immune responses to virus infections [30,61]. In this study, we aimed to characterize the OAS family genes in the Chinese tree shrew, which was proposed to be an promising alternative experimental animal to primates in biomedical research [5,6,62] and has been used for creating animal models of viral infections [9,11,13–15]. We identified 4 *tOASs* (*tOAS1*, *tOAS2*, *tOASL1* and *tOASL2*; Table 1) in the Chinese tree shrew. In general, the tOASs exhibited a high sequence identity to mammalian OASs (Tables S3–S5) and there were no positive selection for these genes in the tree shrew lineage (Table S6). These results suggested that OASs are relatively conservative in the Chinese tree shrew. However, the *OAS* family genes of the Chinese tree shrew also had some unique features. First, compared to human and mouse, tOAS3 was not found in the Chinese tree shrew genome (Fig. S2); this gene was also lost in the pig and cattle genomes [63]. As previous studies showed that OAS3 had a higher affinity for dsRNA than OAS1 and OAS2, and could activate the RNase L during virus infections [64,65], the absence of tOAS3 might affect the recognition and elimination of viruses by the Chinese tree shrew and/or there was a functional replacement for the lost tOAS3, similar to the loss of RIG-I in this animal [25]. Second, tOASL1 had a distant affinity with OASL1 of primates (Fig. S4). This result was inconsistent with the recognized species tree [2] and the phylogenetic clustering patterns of OAS1 and OAS2. Third, the quantification of mRNA levels of *tOASs* showed a tissue-specific pattern (Fig. 3). Why the basal mRNA levels of *tOAS2* and *tOASL1* are higher in liver relative to other tissues, and whether these two genes would confer susceptibility to the infection of HBV and HCV in tree shrew [9,11] are open questions that deserve further focused study.

The expression of OASs was usually up-regulated upon virus infections and resulted in a suppression of viral replications [33,36,59]. It has been demonstrated that OAS could be induced by a variety of viruses [58,66]. Similarly, tOASs were significantly induced in tree shrew renal cells upon virus infections, including HSV-1, SeV, NDV, VSV and AIV, but the induction had a seemingly late onset (Fig. 4). We speculated that the delayed induction of *tOAS* mRNA expression might share a similar mechanism to the delayed upregulation of *tIFNB1* mRNA expression in response to viral infections due to the absence of RIG-I as described in our previous study [25].

The OAS proteins had been reported to share closely related structural and enzymatic features with cGAS and function as nucleic acid sensors to constrain viral propagation [36,67]. Previous studies had shown that human OAS proteins were mainly localized in the cytoplasm and interacted with viral dsRNA [58,68]. Similar to human OAS proteins, mouse OAS1B, chicken OASL, duck OASL and goose OASL were also localized in the cytoplasm in resting cells [69,70]. Cellular localization of human OAS3 in resting cells remains controversial, as there was a report that human OAS3 was localized in the cytoplasm [68], but others showed that human OAS3 could be found in the nucleus [71]. We found that tOASs proteins were evenly distributed in the cytoplasm of tree shrew renal cells, irrespective of DNA virus and RNA virus infections (Fig. 5). In virus-infected cells, replication of viral RNA mainly occurs in the cytoplasm [72]. As cellular PRRs, OAS proteins can bind and be activated by cytoplasmic viral dsRNA [31,73]. Therefore, our result was compatible with the suggestion that tOASs may be nucleic acid sensors and directly inhibit virus replication in the cytoplasm [36].

The OASs inhibited viral replication through the RNase L- or RIG-I-dependent signaling pathway [33,43]. Besides the antiviral activity mediated by the enzymatic activity to generate 2-5A, OASs were also involved in many cellular processes, such as cell growth, apoptosis and gene expression regulation [30,74]. For instance, hOASL and mOasl1 were devoid of the enzymatic activity to generate 2-5A, but had two repeats of ubiquitin-like domains (UBL) at the C-terminal [30,42]. hOASL could enhance the RIG-I-mediated antiviral signaling by interacting with RIG-I and promoting the sensitivity of RIG-I activation via its C-terminal ubiquitin-like domain [43]. mOASL1 bound to the 5′ UTR of *IRF7* and inhibited its translation, thus leading to a feedback of the IFN induction but mOASL2 had a similar antiviral activity to hOASL [43,44]. Therefore, the enzymatic activity and UBL domains are critical for antiviral activity of the OASs proteins. In this study, we found that tOAS1, tOAS2 and tOASL2 had conserved NTase domains which were required for OAS enzyme activity. In addition, tOASL1 and tOASL2 had two C-terminal UBL repeats (Fig. S1). We found that tOAS1 and tOAS2 exerted its anti-HSV-1 activity through the RNase L-dependent signaling pathway, while the roles of tOASL1 and tOASL2 were independent on the classical OAS/RNase L pathway (Fig. 7). This result indicated a diverse role of tOASs in counteracting virus infections. Recent studies showed that OASL exhibits antiviral activity by enhancing innate immunity through interaction with RIG-I or MDA5 [43,75]. Considering the fact that RIG-I was lost and MDA5 had a substitute function in the Chinese tree shrew [25], it would be worthwhile to perform further studies to determine whether tOASL1 and tOASL2 are enzyme-inactive and can function as a positive regulator by interacting with tMDA5, tMAVS or some other key factors in the RLR signaling pathway.

In short, we characterized the *OAS* family genes in the Chinese tree shrew and confirmed their antiviral activities. The updated information about *OAS* in the Chinese tree shrew is undoubtedly essential in the context of evolution of the OAS family genes in mammals and will offer basic knowledge for creating tree shrew animal models of virus infections.

Conflicts of interest

The authors declare no conflict of interest.

Acknowledgments

This study was supported by the National Natural Science Foundation of China (U1402224 to Y-GY and 31601010 to YF), Yunnan Province (2016FB028 to LX) and the Chinese Academy of Sciences (CAS zsys-02 and the CAS Western Light program (中科院西部之光计划) to LX).

Appendix A. Supplementary material

Supplementary data to this article can be found online at https://doi.org/10.1016/j.cyto.2018.11.009.

References

[1] E. Fuchs, S. Corbach-Söhle, Tree Shrews, The UFAW Handbook on the Care and Management of Laboratory and Other Research Animals, Wiley-Blackwell, Oxford, 2010, pp. 262–275.
[2] Y. Fan, Z.Y. Huang, C.C. Cao, C.S. Chen, Y.X. Chen, D.D. Fan, J. He, H.L. Hou, L. Hu, X.T. Hu, X.T. Jiang, R. Lai, Y.S. Lang, B. Liang, S.G. Liao, D. Mu, Y.Y. Ma, Y.Y. Niu, X.Q. Sun, J.Q. Xia, J. Xiao, Z.Q. Xiong, L. Xu, L. Yang, Y. Zhang, W. Zhao, X.D. Zhao, Y.T. Zheng, J.M. Zhou, Y.B. Zhu, G.J. Zhang, J. Wang, Y.G. Yao, Genome of the Chinese tree shrew, Nat. Commun. 4 (2013) 1426.
[3] L. Xu, Y. Fan, X.L. Jiang, Y.G. Yao, Molecular evidence on the phylogenetic position of tree shrews, Zool. Res. 34 (2) (2013) 70–76.
[4] L. Xu, S.Y. Chen, W.H. Nie, X.L. Jiang, Y.G. Yao, Evaluating the phylogenetic position of Chinese tree shrew (*Tupaia belangeri chinensis*) based on complete mitochondrial genome: implication for using tree shrew as an alternative experimental animal to primates in biomedical research, J. Genet Genom. 39 (3) (2012) 131–137.
[5] Y.G. Yao, Creating animal models, why not use the Chinese tree shrew (*Tupaia belangeri chinensis*)? Zool. Res. 38 (3) (2017) 118–126.
[6] Y.T. Zheng, Y.G. Yao, L. Xu, Basic Biology and Disease Models of Tree Shrews, Technology Press, Kunming, China, 2014.
[7] Y.Z. Peng, Z.Z. Ye, R.J. Zou, Y.X. Wang, B.P. Tian, Y.Y. Ma, L.M. Shi, Biology of Chinese Tree Shrews (*Tupaia belangeri chinensis*), Yunnan Science and Technology Press, Kunming, China, 1991.
[8] J. Kock, M. Nassal, S. MacNelly, T.F. Baumert, H.E. Blum, F. von Weizsacker, Efficient infection of primary tupaia hepatocytes with purified human and woolly monkey hepatitis B virus, J. Virol. 75 (11) (2001) 5084–5089.
[9] R.Q. Yan, J.J. Su, D.R. Huang, Y.C. Gan, C. Yang, G.H. Huang, Human hepatitis B virus and hepatocellular carcinoma. I. Experimental infection of tree shrews with hepatitis B virus, J. Cancer Res. Clin. Oncol. 122 (5) (1996) 283–288.
[10] W.N. Guo, B. Zhu, L. Ai, D.L. Yang, B.J. Wang, Animal models for the study of hepatitis B virus infection, Zool. Res. 39 (1) (2018) 25–31.
[11] Y. Amako, K. Tsukiyama-Kohara, A. Katsume, Y. Hirata, S. Sekiguchi, Y. Tobita, Y. Hayashi, T. Hishima, N. Funata, H. Yonekawa, M. Kohara, Pathogenesis of hepatitis C virus infection in *Tupaia belangeri*, J. Virol. 84 (1) (2010) 303–311.
[12] A. Rosen, H. Gelderblom, G. Darai, Transduction of virulence in herpes simplex virus type 1 from a pathogenic to an apathogenic strain by a cloned viral DNA fragment, Med. Microbiol. Immunol. 173 (5) (1985) 257–278.
[13] L. Li, Z. Li, E. Wang, R. Yang, Y. Xiao, H. Han, F. Lang, X. Li, Y. Xia, F. Gao, Q. Li, N.W. Fraser, J. Zhou, Herpes simplex virus 1 infection of tree shrews differs from that of mice in the severity of acute infection and viral transcription in the peripheral nervous system, J. Virol. 90 (2) (2015) 790–804.
[14] J.P. Li, Y. Liao, Y. Zhang, J.J. Wang, L.C. Wang, K. Feng, Q.H. Li, L.D. Liu, Experimental infection of tree shrews (*Tupaia belangeri*) with Coxsackie virus A16, Zool. Res. 35 (6) (2014) 485–491.
[15] Z.F. Yang, J. Zhao, Y.T. Zhu, Y.T. Wang, R. Liu, S.S. Zhao, R.F. Li, C.G. Yang, J.Q. Li, N.S. Zhong, The tree shrew provides a useful alternative model for the study of influenza H1N1 virus, Virol. J. 10 (2013) 111.
[16] S.A. Li, W.H. Lee, Y. Zhang, Two bacterial infection models in tree shrew for evaluating the efficacy of antimicrobial agents, Zool. Res. 33 (1) (2012) 1–6.
[17] G. Li, R. Lai, G. Duan, L.B. Lyu, Z.Y. Zhang, H. Liu, X. Xiang, Isolation and identification of symbiotic bacteria from the skin, mouth, and rectum of wild and captive tree shrews, Zool. Res. 35 (6) (2014) 492–499.
[18] G.Z. Ge, H.J. Xia, B.L. He, H.L. Zhang, W.J. Liu, M. Shao, C.Y. Wang, J. Xiao, F. Ge, F.B. Li, Y. Li, C. Chen, Generation and characterization of a breast carcinoma model by PyMT overexpression in mammary epithelial cells of tree shrew, an animal close to primates in evolution, Int. J. Cancer 138 (3) (2016) 642–651.
[19] L.P. Jiang, Q.S. Shen, C.P. Yang, Y.B. Chen, Establishment of basal cell carcinoma animal model in Chinese tree shrew (*Tupaia belangeri chinensis*), Zool. Res. 38 (4) (2017) 180–190.
[20] L. Zhang, X. Wu, S. Liao, Y. Li, Z. Zhang, Q. Chang, R. Xiao, B. Liang, Tree shrew (*Tupaia belangeri chinensis*), a novel non-obese animal model of non-alcoholic fatty liver disease, Biol. Open 5 (10) (2016) 1545–1552.
[21] Y. Fan, R. Luo, L.Y. Su, Q. Xiang, D. Yu, L. Xu, J.Q. Chen, R. Bi, D.D. Wu, P. Zheng, Y.G. Yao, Does the genetic feature of the Chinese tree shrew (*Tupaia belangeri chinensis*) support its potential as a viable model for Alzheimer's disease research? J. Alzheimers Dis. 61 (3) (2018) 1015–1028.
[22] C.H. Li, L.Z. Yan, W.Z. Ban, Q. Tu, Y. Wu, L. Wang, R. Bi, S. Ji, Y.H. Ma, W.H. Nie, L.B. Lv, Y.G. Yao, X.D. Zhao, P. Zheng, Long-term propagation of tree shrew spermatogonial stem cells in culture and successful generation of transgenic offspring, Cell Res. 27 (2) (2017) 241–252.
[23] W.M. Schneider, M.D. Chevillotte, C.M. Rice, Interferon-stimulated genes: a complex web of host defenses, Annu. Rev. Immunol. 32 (2014) 513–545.
[24] S. Akira, S. Uematsu, O. Takeuchi, Pathogen recognition and innate immunity, Cell 124 (4) (2006) 783–801.
[25] L. Xu, D. Yu, Y. Fan, L. Peng, Y. Wu, Y.G. Yao, Loss of RIG-I leads to a functional replacement with MDA5 in the Chinese tree shrew, Proc. Natl. Acad. Sci. USA. 113 (39) (2016) 10950–10955.
[26] D. Yu, Y. Wu, L. Xu, Y. Fan, L. Peng, M. Xu, Y.G. Yao, Identification and characterization of toll-like receptors (TLRs) in the Chinese tree shrew (*Tupaia belangeri*

chinensis), Dev. Comp. Immunol. 60 (2016) 127–138.
[27] T. Kawai, S. Akira, The roles of TLRs, RLRs and NLRs in pathogen recognition, Int. Immunol. 21 (4) (2009) 317–337.
[28] N. Yan, Z.J. Chen, Intrinsic antiviral immunity, Nat. Immunol. 13 (3) (2012) 214–222.
[29] J. Chebath, P. Benech, A. Hovanessian, J. Galabru, M. Revel, Four different forms of interferon-induced 2′,5′-oligo(A) synthetase identified by immunoblotting in human cells, J. Biol. Chem. 262 (8) (1987) 3852–3857.
[30] J. Justesen, R. Hartmann, N.O. Kjeldgaard, Gene structure and function of the 2′-5′-oligoadenylate synthetase family, Cell. Mol. Life Sci. 57 (11) (2000) 1593–1612.
[31] R.H. Silverman, Viral encounters with 2′,5′-oligoadenylate synthetase and RNase L during the interferon antiviral response, J. Virol. 81 (23) (2007) 12720–12729.
[32] J. Lohofener, N. Steinke, P. Kay-Fedorov, P. Baruch, A. Nikulin, S. Tishchenko, D.J. Manstein, R. Fedorov, The activation mechanism of 2′-5′-oligoadenylate synthetase gives new insights into OAS/cGAS triggers of innate immunity, Structure 23 (5) (2015) 851–862.
[33] H. Kristiansen, H.H. Gad, S. Eskildsen-Larsen, P. Despres, R. Hartmann, The oligoadenylate synthetase family: an ancient protein family with multiple antiviral activities, J. Interferon Cytokine Res. 31 (1) (2011) 41–47.
[34] A. Zhou, B.A. Hassel, R.H. Silverman, Expression cloning of 2–5A-dependent RNAase: a uniquely regulated mediator of interferon action, Cell 72 (5) (1993) 753–765.
[35] B. Dong, L. Xu, A. Zhou, B.A. Hassel, X. Lee, P.F. Torrence, R.H. Silverman, Intrinsic molecular activities of the interferon-induced 2–5A-dependent RNase, J. Biol. Chem. 269 (19) (1994) 14153–14158.
[36] V. Hornung, R. Hartmann, A. Ablasser, K.P. Hopfner, OAS proteins and cGAS: unifying concepts in sensing and responding to cytosolic nucleic acids, Nat. Rev. Immunol. 14 (8) (2014) 521–528.
[37] R. Hartmann, J. Justesen, S.N. Sarkar, G.C. Sen, V.C. Yee, Crystal structure of the 2′-specific and double-stranded RNA-activated interferon-induced antiviral protein 2′-5′-oligoadenylate synthetase, Mol. Cell 12 (5) (2003) 1173–1185.
[38] S. Eskildsen, J. Justesen, M.H. Schierup, R. Hartmann, Characterization of the 2′-5′-oligoadenylate synthetase ubiquitin-like family, Nucleic Acids Res. 31 (12) (2003) 3166–3173.
[39] S. Torralba, J. Sojat, R. Hartmann, 2′-5′ oligoadenylate synthetase shares active site architecture with the archaeal CCA-adding enzyme, Cell. Mol. Life Sci. 65 (16) (2008) 2613–2620.
[40] N. Kon, R.J. Suhadolnik, Identification of the ATP binding domain of recombinant human 40-kDa 2′,5′-oligoadenylate synthetase by photoaffinity labeling with 8-azido-[alpha-32P]ATP, J. Biol. Chem. 271 (33) (1996) 19983–19990.
[41] S.N. Sarkar, A. Ghosh, H.W. Wang, S.S. Sung, G.C. Sen, The nature of the catalytic domain of 2′-5′-oligoadenylate synthetases, J. Biol. Chem. 274 (36) (1999) 25535–25542.
[42] J. Zhu, A. Ghosh, S.N. Sarkar, OASL-a new player in controlling antiviral innate immunity, Curr. Opin. Virol. 12 (2015) 15–19.
[43] J. Zhu, Y. Zhang, A. Ghosh, R.A. Cuevas, A. Forero, J. Dhar, M.S. Ibsen, J.L. Schmid-Burgk, T. Schmidt, M.K. Ganapathiraju, T. Fujita, R. Hartmann, S. Barik, V. Hornung, C.B. Coyne, S.N. Sarkar, Antiviral activity of human OASL protein is mediated by enhancing signaling of the RIG-I RNA sensor, Immunity 40 (6) (2014) 936–948.
[44] M.S. Lee, B. Kim, G.T. Oh, Y.J. Kim, OASL1 inhibits translation of the type I interferon-regulating transcription factor IRF7, Nat. Immunol. 14 (4) (2013) 346–355.
[45] C.S. Thakur, B.K. Jha, B. Dong, J. Das Gupta, K.M. Silverman, H. Mao, H. Sawai, A.O. Nakamura, A.K. Banerjee, A. Gudkov, R.H. Silverman, Small-molecule activators of RNase L with broad-spectrum antiviral activity, Proc. Natl. Acad. Sci. USA 104 (23) (2007) 9585–9590.
[46] D. Yu, L. Xu, X.H. Liu, Y. Fan, L.B. Lu, Y.G. Yao, Diverse interleukin-7 mRNA transcripts in Chinese tree shrew (*Tupaia belangeri chinensis*), PLoS One 9 (6) (2014) e99859.
[47] L. Xu, D. Yu, L. Peng, Y. Fan, J. Chen, Y.T. Zheng, C. Wang, Y.G. Yao, Characterization of a MAVS ortholog from the Chinese tree shrew (*Tupaia belangeri chinensis*), Dev. Comp. Immunol. 52 (1) (2015) 58–68.
[48] Y. Fan, D. Yu, Y.G. Yao, Tree shrew database (TreeshrewDB): a genomic knowledge base for the Chinese tree shrew, Sci. Rep. 4 (2014) 7145.
[49] R.C. Edgar, MUSCLE: multiple sequence alignment with high accuracy and high throughput, Nucl. Acids Res. 32 (5) (2004) 1792–1797.
[50] K. Tamura, G. Stecher, D. Peterson, A. Filipski, S. Kumar, MEGA6: molecular evolutionary genetics analysis version 6.0, Mol. Biol. Evol. 30 (12) (2013) 2725–2729.
[51] Y. Fan, D.D. Yu, Y.G. Yao, Positively selected genes of the Chinese tree shrew (*Tupaia belangeri chinensis*) locomotion system, Zool. Res. 35 (3) (2014) 240–248.
[52] Z. Yang, PAML 4: phylogenetic analysis by maximum likelihood, Mol. Biol. Evol. 24 (8) (2007) 1586–1591.
[53] J. Zhang, R. Nielsen, Z. Yang, Evaluation of an improved branch-site likelihood method for detecting positive selection at the molecular level, Mol. Biol. Evol. 22 (12) (2005) 2472–2479.
[54] S. Kakuta, S. Shibata, Y. Iwakura, Genomic structure of the mouse 2′,5′-oligoadenylate synthetase gene family, J. Interferon Cytokine Res. 22 (9) (2002) 981–993.
[55] E. Elkhateeb, H.T. Tag-El-Din-Hassan, N. Sasaki, D. Torigoe, M. Morimatsu, T. Agui, The role of mouse 2′,5′-oligoadenylate synthetase 1 paralogs, Infect. Genet. Evol. 45 (2016) 393–401.
[56] I. Letunic, T. Doerks, P. Bork, SMART: recent updates, new developments and status in 2015, Nucl. Acids Res. 43 (Database issue) (2015) D257–D260.
[57] A.G. Hovanessian, J. Justesen, The human 2′-5′ oligoadenylate synthetase family: unique interferon-inducible enzymes catalyzing 2′-5′ instead of 3′-5′ phosphodiester bond formation, Biochimie 89 (6–7) (2007) 779–788.
[58] R.J. Lin, H.P. Yu, B.L. Chang, W.C. Tang, C.L. Liao, Y.L. Lin, Distinct antiviral roles for human 2′,5′-oligoadenylate synthetase family members against dengue virus infection, J. Immunol. 183 (12) (2009) 8035–8043.
[59] U.Y. Choi, J.S. Kang, Y.S. Hwang, Y.J. Kim, Oligoadenylate synthase-like (OASL) proteins: dual functions and associations with diseases, Exp. Mol. Med. 47 (2015) e144.
[60] A.J. Sadler, B.R. Williams, Interferon-inducible antiviral effectors, Nat. Rev. Immunol. 8 (7) (2008) 559–568.
[61] W.K. Roberts, A. Hovanessian, R.E. Brown, M.J. Clemens, I.M. Kerr, Interferon-mediated protein kinase and low-molecular-weight inhibitor of protein synthesis, Nature 264 (5585) (1976) 477–480.
[62] L. Xu, Y. Zhang, B. Liang, L.B. Lu, C.S. Chen, Y.B. Chen, J.M. Zhou, Y.G. Yao, Tree shrews under the spot light: emerging model of human diseases, Zool. Res. 34 (2) (2013) 59–69.
[63] A.A. Perelygin, A.A. Zharkikh, S.V. Scherbik, M.A. Brinton, The mammalian 2′-5′ oligoadenylate synthetase gene family: evidence for concerted evolution of paralogous Oas1 genes in Rodentia and Artiodactyla, J. Mol. Evol. 63 (4) (2006) 562–576.
[64] M.S. Ibsen, H.H. Gad, K. Thavachelvam, T. Boesen, P. Despres, R. Hartmann, The 2′-5′-oligoadenylate synthetase 3 enzyme potently synthesizes the 2′-5′-oligoadenylates required for RNase L activation, J. Virol. 88 (24) (2014) 14222–14231.
[65] Y. Li, S. Banerjee, Y. Wang, S.A. Goldstein, B. Dong, C. Gaughan, R.H. Silverman, S.R. Weiss, Activation of RNase L is dependent on OAS3 expression during infection with diverse human viruses, Proc. Natl. Acad. Sci. USA 113 (8) (2016) 2241–2246.
[66] J. Melchjorsen, H. Kristiansen, R. Christiansen, J. Rintahaka, S. Matikainen, S.R. Paludan, R. Hartmann, Differential regulation of the OASL and OAS1 genes in response to viral infections, J. Interferon Cytokine Res. 29 (4) (2009) 199–207.
[67] H. Kristiansen, C.A. Scherer, M. McVean, S.P. Iadonato, S. Vends, K. Thavachelvam, T.B. Steffensen, K.A. Horan, T. Kuri, F. Weber, S.R. Paludan, R. Hartmann, Extracellular 2′-5′ oligoadenylate synthetase stimulates RNase L-independent antiviral activity: a novel mechanism of virus-induced innate immunity, J. Virol. 84 (22) (2010) 11898–11904.
[68] D. Rebouillat, A. Hovnanian, I. Marie, A.G. Hovanessian, The 100-kDa 2′,5′-oligoadenylate synthetase catalyzing preferentially the synthesis of dimeric pppA2′p5′A molecules is composed of three homologous domains, J. Biol. Chem. 274 (3) (1999) 1557–1565.
[69] H.T. Tag-El-Din-Hassan, M. Morimatsu, T. Agui, Functional analysis of duck, goose, and ostrich 2′-5′-oligoadenylate synthetase, Infect. Genet. Evol. 62 (2018) 220–232.
[70] H.T. Tag-El-Din-Hassan, N. Sasaki, K. Moritoh, D. Torigoe, A. Maeda, T. Agui, The chicken 2′-5′ oligoadenylate synthetase A inhibits the replication of West Nile virus, Jpn. J. Vet. Res. 60 (2–3) (2012) 95–103.
[71] L. Malaguarnera, G. Nunnari, M. Di Rosa, Nuclear import sequence identification in hOAS3 protein, Inflamm. Res. 65 (11) (2016) 895–904.
[72] J.A. den Boon, A. Diaz, P. Ahlquist, Cytoplasmic viral replication complexes, Cell Host Microbe 8 (1) (2010) 77–85.
[73] J. Donovan, M. Dufner, A. Korennykh, Structural basis for cytosolic double-stranded RNA surveillance by human oligoadenylate synthetase 1, Proc. Natl. Acad. Sci. USA 110 (5) (2013) 1652–1657.
[74] A. Zhou, J. Paranjape, T.L. Brown, H. Nie, S. Naik, B. Dong, A. Chang, B. Trapp, R. Fairchild, C. Colmenares, R.H. Silverman, Interferon action and apoptosis are defective in mice devoid of 2′,5′-oligoadenylate-dependent RNase L, EMBO J. 16 (21) (1997) 6355–6363.
[75] L.F. Li, J. Yu, Y. Zhang, Q. Yang, Y. Li, L. Zhang, J. Wang, S. Li, Y. Luo, Y. Sun, H.J. Qiu, Interferon-inducible oligoadenylate synthetase-like protein acts as an antiviral effector against classical swine fever virus via the MDA5-mediated type I interferon-signaling pathway, J. Virol. 91 (11) (2017) e01514–e1516.